Available online at www.sciencedirect.com
ScienceDirect
Proceedings of the Combustion Institute 32 (2009) 1219–1226
Proceedings of the Combustion Institute
www.elsevier.com/locate/proci

Diffusion-flame extinction on a rotating porous-disk burner

Javier Urzay [a,*], Vedha Nayagam [b], Forman A. Williams [a]

[a] Department of Mechanical and Aerospace Engineering and Center for Energy Research, University of California San Diego, 9500 Gilman Drive, La Jolla, CA 92093-0411, USA
[b] National Center for Space Exploration Research, NASA Glenn Research Center, Cleveland, OH 44135, USA

Abstract

Flames advected by swirling flows are subject to large strain rates that may cause local extinction. In this investigation, a porous-disk burner is spun at a constant angular velocity in an otherwise quiescent oxidizing atmosphere. Gaseous methane is injected through the disk pores and burns in a flat diffusion flame adjacent to the disk, resulting in a variety of nonpremixed flame patterns for different combinations of the angular velocity and fuel flow rate. The method of activation-energy asymptotics is employed to address the transition from conditions under which a diffusion flame envelops the entire disk to conditions under which diffusion flames are present over only part of the disk, leading to the presence of edge flames. An expression for the extinction Damköhler number as a function of the fuel flow rate and angular velocity is derived and compared with experiments. Agreement is favorable when parameters for a one-step model of methane combustion are employed.

Keywords: Laminar flames; Nonpremixed combustion; Asymptotic analysis; Extinction

1. Introduction

Diffusion flames subject to large rates of strain can develop local extinction, producing quenched regions in which the chemical reaction is nearly frozen. The boundaries so produced are edge flames, which propagate resembling deflagration-like phenomena but exhibit quite special characteristics [1]. The rotating porous-disk burner [2] constitutes a novel device for studying edge-flame propagation near a solid and flame extinction by varying the angular velocity and the rate of injected fuel flow.

The extinction of a counterflow diffusion flame was analyzed thoroughly by Liñán [3] using activation-energy asymptotics (AEA). Four different burning regimes were found in that analysis: the near-equilibrium or diffusion-flame regime which in the first approximation resembles the Burke–Schumann solution, the premixed-flame regime which shows a substantial leakage of one of the reactants, and finally the partial-burning and ignition regimes.

The purpose of this investigation is to analyze, using AEA, the extinction characteristics of the steady, axisymmetric diffusion flame resulting from moderately high rotational burner velocities and small injection fuel flow rates. A remarkable limitation of one-step Arrhenius kinetics with constant activation energy concerns the erroneous

* Corresponding author.
E-mail address: jurzay@ucsd.edu (J. Urzay).

1540-7489/$ - see front matter © 2009 The Combustion Institute. Published by Elsevier Inc. All rights reserved.
doi:10.1016/j.proci.2008.06.016

prediction of dominant fuel leakage in hydrocarbon–air nonpremixed combustion. In the present analysis, a similar type of chemical-kinetic model is used, but regimes of dominant oxidizer leakage are found at sufficiently small fuel flow rates when the flame is very close to the disk surface and the steep temperature gradient on the fuel side enhances oxidizer leakage. This analysis represents a fundamental step towards the understanding of more complex patterns of flames embedded in von Kármán swirling flows [4], some of which have been addressed earlier [5,6] by using one-dimensional edge-flame models without clarifying information on the burning regime and flow-field effects.

The present analysis differs from previous studies of similar problems on solid fuel disks [7,8], in that the variable fuel flow rate is specified rather than being coupled to an energy equation through a transfer number.

2. Experiments

The experiments used a sintered bronze, water-cooled porous disk of radius a, thickness L, and porosity φ. Gaseous methane was fed to the disk with uniform and constant fuel flow rate $\dot{m}$ from a compressed-gas bottle of fuel mass fraction $Y_{F,F}$, and injection temperature T_S, which for simplicity is assumed to be equal to the disk cooling temperature. The exposed disk porous surface was oriented facing downward in an otherwise quiescent oxidizing atmosphere of oxidizer mass fraction $Y_{O_2,A}$, and temperature T_∞, and it was spun at a constant angular velocity Ω, as depicted in Fig. 1. Further details on the experimental set-up are given by Nayagam [2].

Figure 2a shows a flame-pattern map resulting from the experiments [2]. At moderate fuel injection rates, as Ω is increased the axisymmetric diffusion flame develops a pulsating flame hole. This mode has been studied in earlier work [9,10] for

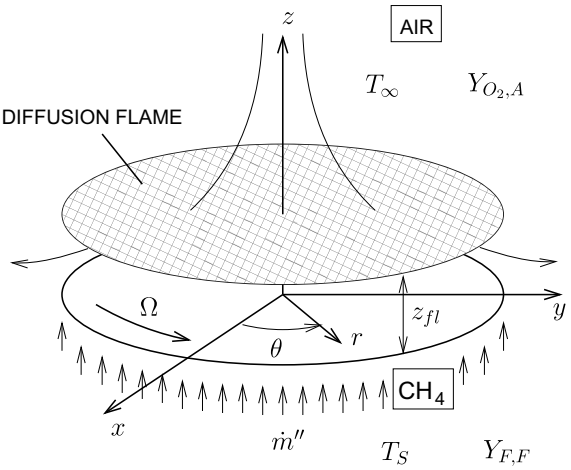

Fig. 1. Burner schematics.

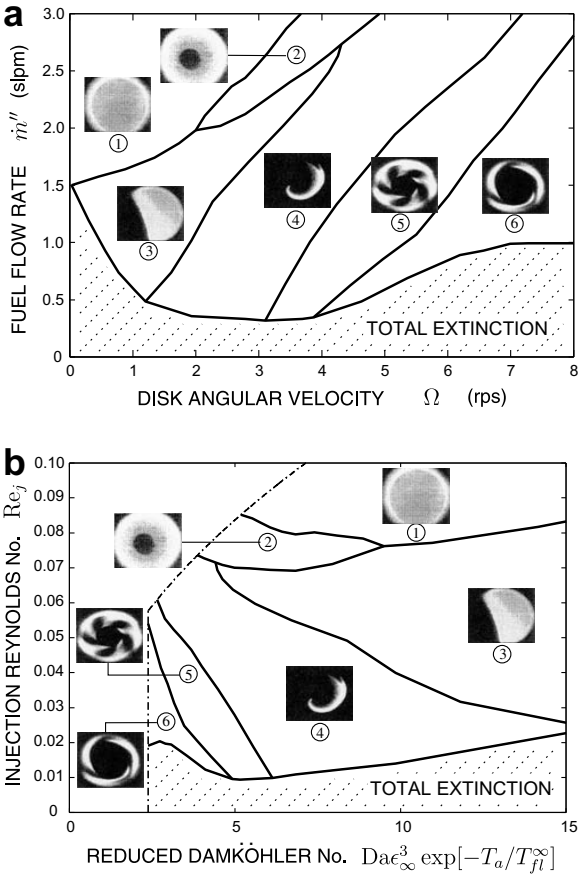

Fig. 2. (a) Dimensional and (b) nondimensionalized flame-pattern maps and observational limits (dot–dashed lines). Observed flame patterns are (1) steady, axisymmetric burning regime, (2) diffusion-flame holes, (3) straight, quenched fronts, (4) single-armed spiral flame, (5) multi-armed spiral flame, and (6) flame rings. The reduced Damköhler number is based on a characteristic value of the activation temperature $T_a = 18{,}000$ K.

counterflow flames. An increase in Ω causes transition to a single-armed, counter-rotating spiral flame, with characteristics similar to those of the spiral flames observed in burning solid fuels as described elsewhere [4]. Further increase in Ω causes transition to flame modes such as multi-armed spirals and flame rings, which are certainly influenced by edge effects. The flame is finally blown off the disk at higher Ω. Total flame extinction may be achieved for sufficiently small $\dot{m}$ or high Ω. Disk water-cooling ensures that the observed patterns are not caused or stabilized by thermal inertial effects of the disk. The downward-facing arrangement favors a flat flame, buoyant instabilities being suppressed by the closeness of the flame to the disk.

3. Formulation

At moderately high Reynolds numbers, as the burner rotates the viscous effects are confined to

a thin boundary layer of approximate thickness $\delta_M = (\nu/\Omega)^{1/2}$, where ν is the coefficient of kinematic viscosity. Fluid in this layer is carried by the disk surface through friction and is ejected outward centrifugally. This radial mass flow is compensated by an axial fluid entrainment. Typical values of the mixing-layer thickness δ_M for this problem are of order 1 mm. At small fuel injection velocities, the radial and azimuthal velocity components u and v are of order Ωr, while mass conservation yields the ordering $(\nu\Omega)^{1/2}$ for the normal component w. The ratio of the characteristic flow time Ω^{-1} to the residence time in the boundary-layer region of the injected fuel $\rho\delta_M/\dot{m}''$ is the local Reynolds number of injection,

$$\mathrm{Re_j} = \dot{m}''\delta_M/\mu, \tag{1}$$

which typically is a small parameter in these experiments. In this formulation, $\dot{m}''$ is the fuel mass flow rate per unit surface area and $\mu = \rho\nu$ is the coefficient of dynamic viscosity, where ρ denotes the density of the gas.

The chemical reaction is considered to be a single-step, second-order irreversible reaction between methane and the oxygen of the air,

$$CH_4 + 2O_2 \rightarrow CO_2 + 2H_2O + Q, \tag{2}$$

with a global rate of reaction

$$\omega = \hat{A} W_F^{-1} \rho Y_F Y_{O_2} \mathrm{e}^{-T_a/T}, \tag{3}$$

where $\hat{A} = \rho A/W_{O_2}$ is an appropriately modified frequency factor, with A the preexponential factor and W_F and W_{O_2} molecular weights of each reactant. The mass of oxidizer burnt per unit mass of fuel consumed in stoichiometric proportions is $s = 2W_{O_2}/W_F \approx 4$, and the mass of the fuel feed stream that is needed to mix with a unit mass of air to generate a stoichiometric mixture is $\alpha = Y_{O_2,A}/sY_{F,F} \approx 0.06$ for an undiluted fuel stream, which results in a small value of the stoichiometric mixture fraction $Z_{st} = \alpha/(1+\alpha) \approx 0.056$. This simple model leaves three parameters in the formulation, namely, the preeexponential factor A, the activation temperature T_a, and the heat released per unit mole of fuel, Q. The values $A = 6.9 \times 10^{14}$ cm^3/(mol s) and $Q = 802.4$ kJ/mol have been shown [11] to compare favorably with experiments and detailed-chemistry numerical simulations. The same values are assumed in this study. The activation temperature T_a is treated as a free parameter of the problem to fit the experimental curve of extinction; this is motivated by the need [11] to allow T_a to increase from its value (15,900 K) at stoichiometry with increasing mixture fraction if reasonable predictions of diffusion-flame extinction and oxygen leakage are to be obtained. The ratio of the characteristic flow time Ω^{-1} to the pseudo-collision time $(\hat{A}Y_{O_2,st})^{-1}$ defines the pseudo-collision Damköhler number,

$$\mathrm{Da} = \hat{A}Y_{O_2,st}/\Omega, \tag{4}$$

where $Y_{O_2,st}$ corresponds to the oxidizer mass fraction at stoichiometry in frozen flow. The variables $\mathrm{Re_j}$ and Da given by (1) and (4) are the relevant nondimensional parameters characterizing the rotating-burner experiments for fixed temperature differences $\Delta T = T_\infty - T_S$, since they contain the three characteristic time scales of the problem. Figure 2b shows the transformed experimental data in the ($\mathrm{Re_j}$,Da) plane. In Fig. 2b, $T_{fl}^\infty = T_{st} + QY_{F,st}/c_pW_F$ represents the adiabatic flame temperature and $\epsilon = T_{fl}^2/[T_a(T_{fl}^\infty - T_{st})]$ is the inverse of a Zel'dovich number. In this formulation T_{st} and $Y_{F,st}$ represent the frozen-flow temperature and fuel mass fraction at stoichiometry, and T_{fl} is the flame temperature. Note that $T_{fl} \leqslant T_{fl}^\infty$ due to heat losses to the disk surface, with $T_{fl} \sim T_{fl}^\infty$ for $\mathrm{Re_j} \gg 1$.

Although more involved analyses may be performed, for simplicity the burner is assumed to be rotating in a fluid of constant density and constant thermodynamic properties and transport coefficients. The density ρ, viscosity ν, specific heat c_p, thermal diffusivity D_T and Prandtl number, $\mathrm{Pr} = \nu/D_T$ are taken to be those of the air at normal conditions, and fuel and oxidizer Lewis numbers of unity are assumed. Radiation and buoyancy effects are neglected. The near-extinction conditions of the experiments reduce the maximum temperatures, thereby decreasing the variations of properties and improving the accuracies of these approximations.

In the steady, axisymmetric burning regime, a self-similar stream-function formulation is developed by defining the self-similar coordinate $\eta = z/\delta$ and nondimensionalizing the conservation equations with $(\nu\Omega)^{1/2}r^2/2$ the unit of stream function, $Y_{F,st}$ and $Y_{O_2,st}$ the units of fuel and oxidizer mass fractions respectively, and $QY_{F,st}/(W_Fc_p)$ the unit of temperature. In these variables, the momentum, energy and species conservation equations become

$$\begin{aligned}
&\phi' = \phi''\phi - \phi'^2/2 + 2V^2,\\
&V'' = \phi V' - \phi' V,\\
&T''/Pr - \phi T' = -DaY_{O_2}Y_F \mathrm{e}^{-T_a/T},\\
&Y_F''/Pr - \phi Y_F' = DaY_{O_2}Y_F \mathrm{e}^{-T_a/T},\\
&Y_{O_2}''\Big/Pr - \phi Y_{O_2}' = DaY_{O_2}Y_F \mathrm{e}^{-T_a/T},
\end{aligned} \tag{5}$$

where prime denotes differentiation respect to η, and ϕ and V represent the nondimensional stream function and azimuthal velocity, respectively. The momentum equations, the first two in (5) resemble a von Kármán swirling flow [12] with injection, and in this constant-density approximation they are uncoupled from the energy and species conservation equations. Far from the disk $\eta \rightarrow \infty$, boundary conditions are $\phi \rightarrow \phi_\infty$, $\phi' \rightarrow 0$,

$V \to 0$, $Y_{O_2} \to 1+\alpha$, $Y_F \to 0$ and $T \to T_\infty$, with ϕ_∞ a negative number, dependent on Re_j, denoting the axial fluid entrainment. At the disk surface $\eta = 0$, $\phi = Re_j$, $\phi' = 0$, $V = 1$, and $T = T_S$, whereas the disk porous surface imposes constraints on the oxidizer and fuel diffusion. Fuel and oxidizer mass balances at the disk surface yield two additional boundary conditions at $\eta = 0$, namely

$$Re_j Pr Y_{O_2} = Y'_{O_2},$$
$$\text{and } Pr Y_F - Y'_F/Re_j = Pr(1+\alpha)/\alpha. \tag{6}$$

As further detailed below, sufficiently small fuel flow rates may cause substantial oxidizer leakage through the flame, and non-negligible amounts of oxidizer may penetrate into the disk. The oxidizer boundary condition in (6) is accurate when the pore Reynolds number is sufficiently large that the disk thickness L obeys $L/l_{O_2} \gg 1$, where $l_{O_2} \sim \delta_M \varphi/(Re_j Pr)$ is the oxidizer penetration length into the porous solid. The boundary condition in (6) for the fuel reveals that $Y_F = O(Re_j)$ for $Re_j \ll 1$.

4. Conserved-scalar formulation

The energy and species conservation equations, the last three in (5), can be cast into a convection-free form similar to that of Liñán [3] by defining the coordinate transformation $\widetilde{Z} = \widetilde{Z}(\eta)$ as

$$\widetilde{Z}(\eta) = \widetilde{Z}_{fl}\left(\frac{Y_F - Y_{O_2}}{1+\alpha} + 1\right) = \frac{Pr}{B}\int_\eta^\infty \left\{\exp\left[\int_0^\xi Pr\,\phi(\eta)\,d\eta\right]\right\} d\xi, \tag{7}$$

where

$$B = Pr\int_0^\infty \left\{\exp\left[\int_0^\xi Pr\,\phi(\eta)\,d\eta\right]\right\} d\xi. \tag{8}$$

is an effective mass-transfer number dependent on Re_j, and

$$\widetilde{Z}_{fl} = Z_{st}/Z_S, \tag{9}$$

with $Z_S = Re_j B/(1 + Re_j B)$ the mixture fraction at the disk surface.

The excess enthalpy H is defined as

$$H = \frac{\alpha Y_F + Y_{O_2}}{1+\alpha} - 1 + T - T_\infty, \tag{10}$$

with $H = 0$ in the oxidizer feed stream and $H = H_S$ at the surface of the disk, where H_S is calculated as part of the solution. It is noteworthy to mention that the excess enthalpy H is zero everywhere for an equidiffusive counterflow diffusion flame with equal temperatures of oxidizer and fuel feed streams [3]. However, the excess enthalpy in the present analysis is non-zero even in the case $T_S = T_\infty$ because of heat losses to the disk.

It can be shown that the excess enthalpy is given by $H = -\beta\widetilde{Z}/\widetilde{Z}_{fl}$, where

$$\beta = \frac{\alpha}{1+\alpha}\left(T_\infty - T_S + \frac{q_S}{Re_j Pr}\right), \tag{11}$$

and the conservation equations become

$$Y_F = (1-\beta)\widetilde{Z}/\widetilde{Z}_{fl} + T_\infty - T,$$
$$Y_{O_2} = 1 + \alpha - (\alpha+\beta)\widetilde{Z}/\widetilde{Z}_{fl} + T_\infty - T,$$
$$\frac{\widetilde{\chi}(\widetilde{Z})}{Pr}\frac{d^2T}{d\widetilde{Z}^2} = -Da\,Y_F Y_{O_2} e^{-T_a/T}, \tag{12}$$

In this formulation $q_S = dT/d\eta|_{\eta=0}$ is the heat flux to the disk surface, which depends on the rest of the parameters and the burning regime, and $\widetilde{\chi}(\widetilde{Z}) = (d\widetilde{Z}/d\eta)^2$ is the dimensionless scalar dissipation rate. The dimensional scalar dissipation rate in the flame $\chi_{fl} = D_T \widetilde{\chi}_{fl} Z_S^2/\delta_M^2$ defines the characteristic diffusion length $\ell_d = (D_T/\chi_{fl})^{1/2}$ and the characteristic diffusion time through the flame $t_d = 1/\chi_{fl}$.

The values of B and the entrainment ϕ_∞ are obtained by numerical integration and asymptotic approximation of the momentum equations in (5), the latter approach being carried out by performing the expansions $\phi = \phi_0 + Re_j\phi_1 + O(Re_j^2)$ and $V = V_0 + Re_j V_1 + O(Re_j^2)$ for the stream function and azimuthal velocity, which shows that $B = 2.180 + 2.349 Re_j + O(Re_j^2)$ for $Pr = 0.71$ and $\phi_\infty = -0.884 + 0.202 Re_j + O(Re_j^2)$, both for $Re_j \ll 1$. Figure 3 shows that the expansion is accurate over the range of interest.

5. The Diffusion-flame regime

A diffusion-controlled combustion regime exists for large Damköhler numbers, in which the temperature and composition fields do not depend on the chemical kinetics in the first approximation. In this regime the chemical time $t_c = (\hat{A} Y_{O_2,st})^{-1} e^{T_a/T_{fl}}$ is much shorter than the diffusion time $t_d = 1/\chi_{fl}$, so that the flow remains in chemical equilibrium on both sides of a thin reac-

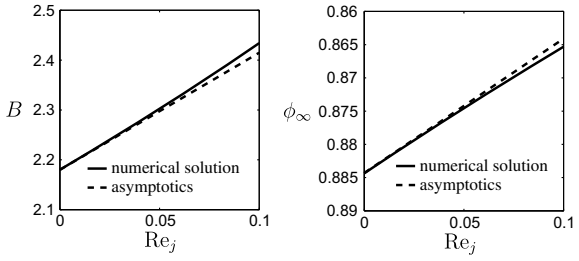

Fig. 3. Numerical axial entrainment ϕ_∞ and effective mass-transfer number B for $Pr = 0.71$, and their asymptotic approximations.

tion sheet of infinitesimal thickness, and no reactant leakage occurs in the first approximation. In the flame-sheet region, the temperature is close to the adiabatic flame temperature. For large activation energies, temperature variations are expected to be of order $\epsilon = T_{\rm fl}^2/T_{\rm a} \ll 1$, which resembles the inverse of a Zel'dovich number. In this formulation $T_{\rm fl}$ is the equilibrium flame temperature in the Burke–Schumann limit or vigorously-burning regime. A reduced Damköhler number Δ, which takes on large values in the Burke–Schumann limit, may then be defined as the ratio of the diffusion time $t_{\rm d}$ to the chemical time $t_{\rm c}$.

To leading order in ϵ, $Y_{\rm F} = Y_{\rm O_2} = 0$ at the thin flame, so that the temperature profiles become

$$T = T_\infty + 1 + \alpha - (\alpha+\beta)\widetilde{Z}/\widetilde{Z}_{\rm fl}, \tag{13}$$

for $\widetilde{Z}_{\rm fl} \leqslant \widetilde{Z} \leqslant 1$ (fuel region), and

$$T = T_\infty + (1-\beta)\widetilde{Z}/\widetilde{Z}_{\rm fl}, \tag{14}$$

for $0 \leqslant \widetilde{Z} \leqslant \widetilde{Z}_{\rm fl}$ (oxidizer region). To leading order, the flame location in the $\widetilde{Z}$ coordinate corresponds to $\widetilde{Z} = \widetilde{Z}_{\rm fl}$. In the flame-sheet region, the equilibrium temperature is close to the adiabatic flame temperature,

$$T_{\rm fl} = T_\infty + 1 - \beta. \tag{15}$$

The equilibrium heat flux to the disk surface $q_{\rm S} = {\rm Pr}(\Delta T + 1 + \alpha)/B$ is obtained by differentiating the fuel-side temperature, which results in a monotonically decreasing heat flux as the injection rate ${\rm Re_j}$ increases. After substituting this result into (11), the value

$$\beta = \frac{\alpha\left[\Delta T\left(1+{\rm Re_j}B\right)+1+\alpha\right]}{(1+\alpha){\rm Re_j}B}, \tag{16}$$

is obtained. It is noteworthy to mention that $H_{\rm fl} = -\beta$ represents the excess enthalpy in the flame. The equilibrium flame temperature $T_{\rm fl}$ is monotonic with ${\rm Re_j}$, with positive and negative slopes for positive and negative values of $T_\infty - T_{\rm S} + 1 + \alpha$, respectively, and it tends asymptotically to the counterflow equilibrium flame temperature $T_{\rm fl}^\infty$ [3] at large ${\rm Re_j}$. For hot disks with $T_{\rm S} - T_\infty = 1 + \alpha$, then $T_{\rm fl} = T_{\rm S}$ independent of ${\rm Re_j}$ since the heat losses to the disk are suppressed.

Note that the Burke–Schumann solution (13) and (14) must satisfy $0 < Z_{\rm st} \leqslant Z_{\rm S}$ for the flame to stand off the disk surface, which gives the minimum-injection rate

$${\rm Re_j^{min}}B^{\rm min} = \alpha, \tag{17}$$

for $Z_{\rm S} = Z_{\rm st}$. The asymptotic expansion of B yields $B^{\rm min} \approx 2.224$, the value of B at ${\rm Re_j} = {\rm Re_j^{min}}$, and the value ${\rm Re_j^{min}} \sim 0.027$ in the second approximation. In the limit ${\rm Re_j} = {\rm Re_j^{min}}$, all of the fuel is consumed upon injection, and since $q_{\rm S}$ remains finite and equal to the chemical heat released in the flame, the flame temperature $T_{\rm fl}$ is found to be equal to the disk temperature $T_{\rm S}$. This limit cannot be attained in experiments since the flame cannot sustain combustion at ordinary disk temperatures $T_{\rm S}$, for which the chemical time $(\hat{A}Y_{\rm O_2,st})^{-1}\,{\rm e}^{T_{\rm a}/T_{\rm S}}$ is much larger than the diffusion time $t_{\rm d}$, and extinction occurs before the flame reaches the wall. Values $Z_{\rm st} > Z_{\rm S}$ represent the flame located somewhere inside the disk, a problem that is not addressed here.

The spatial flame location $\eta_{\rm fl}$, for which $\widetilde{Z} = \widetilde{Z}_{\rm fl}$, is obtained numerically by using the inverse of the transformation (7). For ${\rm Re_j} \ll 1$, $\eta_{\rm fl}$ is expected to be small, so that $\int_{\eta_{\rm fl}}^\infty \exp[\int_0^\xi {\rm Pr}\phi(\eta){\rm d}\eta]\,{\rm d}\xi \sim B/{\rm Pr} - \eta_{\rm fl}$, and the asymptotic approximation

$$\eta_{\rm fl} \sim [{\rm Pr}(1+\alpha)]^{-1}\Big[-\alpha/{\rm Re_j} + 2.180 + 2.349{\rm Re_j} + {\rm O}\Big({\rm Re_j^2}\Big)\Big] \tag{18}$$

is obtained and compared with the numerical values in Fig. 4. Note that the flame is beyond the stagnation plane for ${\rm Re_j} > 0.029$.

The nonequilibrium effects associated with finite-rate chemistry and finite Damkhöhler numbers are expected to cause flame extinction well before the minimum-injection limit is reached. In particular, effects associated with the decrease in Da to cause flame-temperature variations in fractional amounts of order ϵ are now carried out following Liñán [3].

To O(ϵ), both reactants diffuse into a flame region of thickness of $\mathrm{O}(\epsilon\Delta_0^{-1/3}\widetilde{Z}_{\rm fl})$, in which temperature variations are of the same order with respect to the equilibrium temperature $T_{\rm fl}$, and Δ_0 is a reduced Damkhöler number given by the first term of the expansion

$$\frac{4{\rm Pr}\widetilde{Z}_{\rm fl}^2\left(T^2/T_{\rm a}\right)^3}{\widetilde{\chi}_{\rm fl}(1+\alpha)^2}\,{\rm Da}\,{\rm e}^{-T_{\rm a}/T} = \Delta_0 + \epsilon\Delta_1 + {\rm O}(\epsilon^2). \tag{19}$$

Liñán [3] derives a reaction-diffusion equation (with matching conditions) that depends on the parameter

$$\gamma = -1 + 2(\alpha+\beta)/(1+\alpha), \tag{20}$$

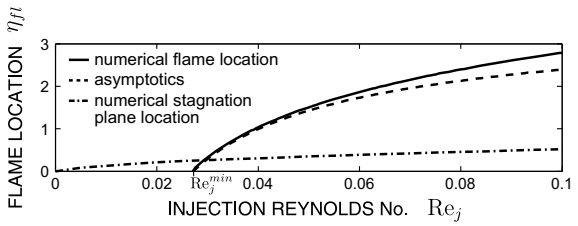

Fig. 4. Numerical flame location $\eta_{\rm fl}$ and its asymptotic approximation (18) for ${\rm Pr} = 0.71$, and numerical stagnation plane location.

with $1-\gamma$ twice the ratio between the heat lost from the flame toward the oxidizer region to the total chemical heat released in the flame. Since β is a function of the boundary temperature difference and the injection mass flow, γ also assumes different values depending on those variables, as depicted in Fig. 5. Extinction occurs only in the region $|\gamma|<1$ and for boundary temperature differences $-(1+\alpha)\leqslant\Delta T\leqslant(1+\alpha)/\alpha$, in the sense that no solution exists for Δ_0 below the extinction Damkhöler number Δ_{0E}. Outside this range of temperatures no abrupt extinction event exists. For $0<\gamma<1$, the temperature gradient is steeper on the fuel side, which in turn freezes the chemical reaction on that side and enhances oxidizer leakage through the flame, with $\gamma\to 1$ reaching an premixed structure with O(1) oxidizer leakage and O(ϵ) fuel leakage. For $-1<\gamma<0$ the temperature gradient is steeper on the oxidizer side and fuel leakage prevails, with $\gamma\to -1$ reaching a premixed structure with O(1) fuel leakage and O(ϵ) oxidizer leakage. Therefore as $|\gamma|\to 1$ the flame region shows a premixed structure, with O(1) leakage of one reactant, and the diffusion-flame regime looses accuracy.

Conventional AEA analysis of nonpremixed counterflow combustion [3] predicts values of γ close to unity and strong fuel leakage when applied to hydrocarbon–air flames, for which Z_{st} is typically small. Since β and γ strongly depend on the fuel injection mass flow $\mathrm{Re_j}$ for the rotating-burner problem, fuel leakage is inhibited for sufficiently small mass flows for which $\gamma=0$, a condition identified by the superscript ★, and the experimental flame is close enough to the disk surface to produce a steeper temperature gradient on the fuel side than the oxidizer side. The value of $\mathrm{Re_j}$ for which $\gamma=0$ is given by

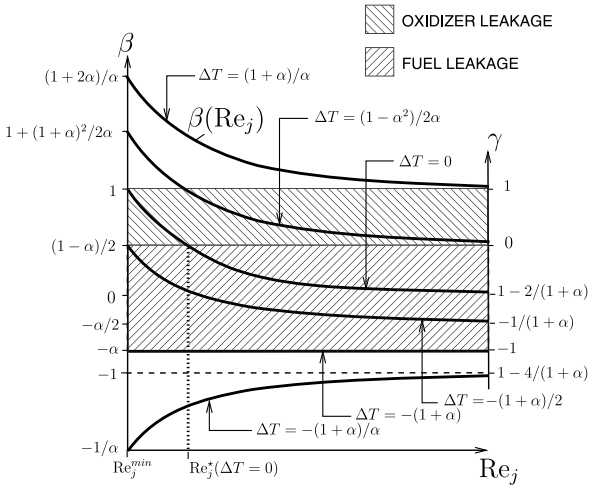

Fig. 5. Sketch of β as a function of $\mathrm{Re_j}$ given by (16) for different ΔT (solid line). The right axis represents the value of γ given by (20) for each particular value of β. In the hatched region $|\gamma|\leqslant 1$ there is abrupt extinction obeying (23).

$$\mathrm{Re_j}B=\frac{2\alpha[1+\Delta T/(1+\alpha)]}{1-\alpha-2\alpha\Delta T/(1+\alpha)}, \tag{21}$$

where use has been made of (16) and (20). For $\mathrm{Re_j}<\mathrm{Re_j^*}$, then $\gamma>0$ and oxidizer leakage is favored. The occurrence of dominant oxidizer leakage when $\mathrm{Re_j}<\mathrm{Re_j^\star}$ is found only for $\Delta T\geqslant -(1+\alpha)/2$. These considerations are shown in Fig. 6 for the particular case $\Delta T=0$.

6. Flame extinction

Analysis [3] shows that reduced Damköhler number at extinction is

$$\Delta_{0\mathrm{E}}=\mathrm{e}\Big[(1-|\gamma|)-(1-|\gamma|)^2+0.26(1-|\gamma|)^3 +0.055(1-|\gamma|)^4\Big], \tag{22}$$

within 1% for $|\gamma|<1$.

Substituting expression (22) into (19) and making use of (7), (8), (15), (18), and (20), and the definitions (4) and (16) the formula for the extinction Damköhler number

$$\mathrm{Da_E}=\frac{\Delta_{0\mathrm{E}}\mathrm{Pr}(1+\alpha)^2\,\mathrm{e}^{T_\mathrm{a}/T_\mathrm{fl}}}{4B^2\widetilde{Z}_\mathrm{fl}^2\left[T_\mathrm{fl}^2/T_\mathrm{a}\right]^3} \times\exp\left[2\int_0^{\eta_\mathrm{fl}}\mathrm{Pr}\phi(\eta)\,\mathrm{d}\eta\right], \tag{23}$$

is found, which defines the extinction conditions in terms of the fuel mass flow rate and the angular velocity for the present experiments. In this for-

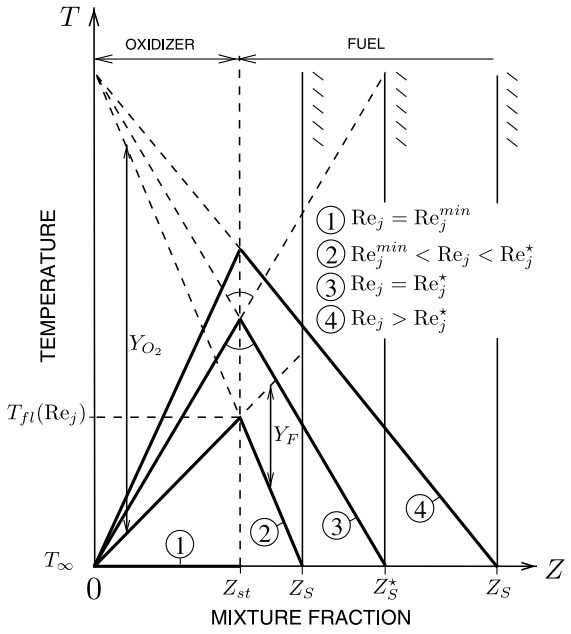

Fig. 6. Asymptotic temperature and reactant mass fractions distributions in the diffusion-flame regime for different ranges of fuel injection mass flows and $T_\infty=T_\mathrm{S}$.

mula, Δ_{0E}, B, $\widetilde{Z}_{fl}$, and T_{fl}, as well as η_{fl} and the function $\phi(\eta)$, depend on Re_j, so that Da_E varies with Re_j.

Figure 7 shows the calculated extinction Damköhler number (23) superimposed on the experimental data of Fig. 2b. Even though the order of magnitude of Da_E does not vary appreciably when the rest of parameters the are changed, the best fit with the experimental curve of transition to the diffusion flame-hole regime occurs for an activation temperature of $T_a = 18{,}000$ K if the disk is kept at the ambient temperature $T_\infty = T_S = 300$ K by water cooling, so that $\Delta T = 0$; this activation temperature is somewhat higher than the activation temperature at stoichiometry (15,900 K) in [11], but instead it corresponds to that at a mixture fraction of $Z = 0.076$, which would lie in the inner region for the values of ϵ encountered here. In that analysis it is shown that an increase of activation energy with the mixture fraction is needed in order to favor oxidizer leakage, which is consistent with the present results.

The threshold value $Re_j^\star$ given by (19) below which oxidizer leakage prevails is found to be $Re_j^\star \sim 0.055$, which as seen in Fig. 7 is much smaller than typical fuel flow rates found in the transition region, so that according to AEA analysis moderate fuel leakage prevails there, rather than the physically correct oxygen leakage, with extinction occurring in the diffusion-flame regime. These observations indicate that it would be of interest to extend the Liñán [3] analysis to allow for variations of T_a in the inner region, to see whether this yields better agreement with experiments.

For constant angular velocity extinction is expected to occur if a minimum threshold of fuel injection is achieved. The system trajectories for $\Omega = \text{const.}$ would be represented by vertical lines $Da = \text{const.}$ in Fig. 2b. As $\dot{m}''$ decreases, the equilibrium temperature decreases producing longer chemical times in the flame, with the combustion process having to take place closer to the disk surface according to Fig. 4. Since the disk surface is kept at a moderate temperature $T_S \sim T_\infty$ by water cooling, flame extinction occurs because of the decreasing amount of fuel and the proximity of the disk cold wall.

For constant fuel flow rates, extinction is expected to occur if a maximum threshold of angular velocity is achieved. The system trajectories for $\dot{m}'' = \text{const.}$ would be represented by parabolas $Re_j \propto Da^{1/2}$ in Fig. 2b. As Ω increases, the mixing thickness δ_M decreases, producing larger scalar dissipation rates χ_{fl} and shorter diffusion times across the flame t_d or flame-transit times. Extinction occurs when the chemical time t_c, which increases as Ω increases, becomes of the same order as the diffusion time t_d.

7. Conclusions

This research has shown that the onset of flame holes in the rotating porous-disk-burner experiments can be described well by one-step AEA in the diffusion-flame regime if a suitable value is selected for the activation temperature. This conclusion suggests that the same type of AEA with the same activation-temperature selection might successfully be applied to address the structures and dynamics of other patterns shown in Fig. 2, such as single spirals, making use of edge-flame formulations [1]. If however, it is desired to predict correctly more detailed aspects of the experiments, such as the occurrence of oxygen rather than fuel leakage, then more ambitious analyses would be required, such as AEA of one-step chemical kinetics with variable activation energy or at least two-step rate-ratio asymptotics [13].

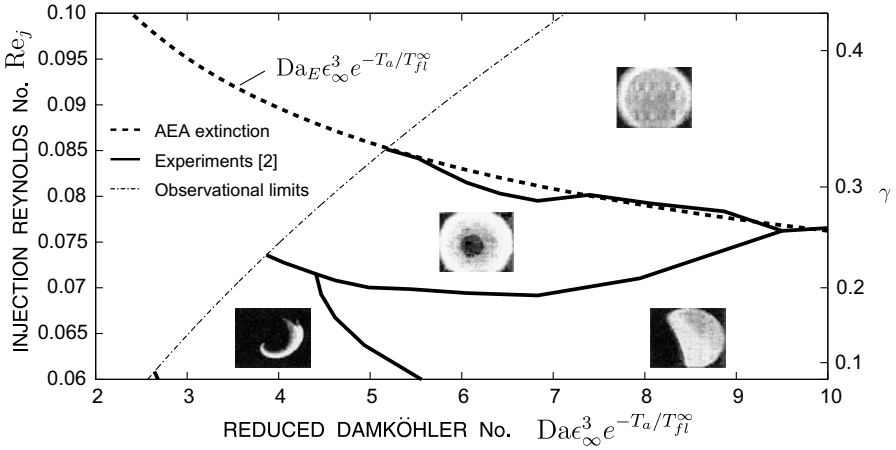

Fig. 7. Extinction Damköhler number Da_E and experimental data, for $Pr = 0.71$, $T_a = 18{,}000$ K, and $T_S = T_\infty = 300$ K.

Acknowledgment

The first author is grateful to Prof. A. Liñán for his thoughtful suggestions and interesting discussions on the subject.

References

[1] J. Buckmaster, *Prog. Energy Combust. Sci.* 28 (2002) 435–475.
[2] V. Nayagam, *Pattern Formation in Diffusion Flames Embedded in von Kármán Swirling Flows*, Tech. Rep. NASA/CR–2006-214057, National Aeronautics and Space Administration, 2006.
[3] A. Liñán, *Acta Astronaut.* 1 (7–8) (1974) 1007–1039.
[4] V. Nayagam, F.A. Williams, *Phys. Rev. Lett.* 84 (3) (2000) 479–482.
[5] V. Nayagam, F.A. Williams, *Combust. Flame* 125 (2000) 974–981.
[6] F.A. Williams, in: F.J. Higuera, J. Jiménez, J.M. Vega (Eds.), *Simplicity, Rigor and Relevance in Fluid Mechanics: A volume in honor of Amable Liñán*, CIMNE, Barcelona, 2004, pp. 61–74.
[7] L. Krishnamurthy, F.A. Williams, K. Seshadri, *Combust. Flame* 26 (1976) 363–377.
[8] V. Nayagam, F.A. Williams, *Proc. Combust. Inst.* 28 (2000) 2875–2881.
[9] V. Nayagam, R. Balasubramaniam, P.D. Ronney, *Combust. Theory Model.* 3 (1999) 727–742.
[10] C. Pantano, D.I. Pullin, *J. Fluid Mech.* 480 (2003) 311–333.
[11] E. Fernández-Tarrazo, A.L. Sánchez, A. Liñán, F.A. Williams, *Combust. Flame* 147 (2006) 32–38.
[12] T. von Kármán, *Z. Angew. Math. Mech.* 1 (1921) 233–252.
[13] K. Seshadri, N. Peters, *Combust. Flame* 73 (1988) 23–44.